ACS APPLIED MATERIALS & INTERFACES

Research Article

Cite This: ACS Appl. Mater. Interfaces 2018, 10, 19162−19172

www.acsami.org

Complex Fluids Confined into Semi-interpenetrated Chemical Hydrogels for the Cleaning of Classic Art: A Rheological and SAXS Study

Michele Baglioni,[‡] Joana A. L. Domingues,[†] Emiliano Carretti, Emiliano Fratini, David Chelazzi, Rodorico Giorgi, and Piero Baglioni*[,‡]

Department of Chemistry "Ugo Schiff" and CSGI, University of Florence, Via della Lastruccia 3, 50019 Sesto Fiorentino, Italy

Supporting Information

ABSTRACT: The removal of aged varnishes from the surface of easel paintings using the common conservation practice (i.e., by means of organic solvents) often causes pigment leaching, paint loss, and varnish redeposition. Recently, we proposed an innovative cleaning system based on semi-interpenetrated polymer networks (SIPNs), where a covalently cross-linked poly(hydroxyethyl methacrylate), pHEMA, network is interpenetrated by linear chains of poly(vinylpyrrolidone), PVP. This chemical gel, simply loaded with water, was designed to safely remove surface dirt from water-sensitive artifacts. Here, we modified the SIPN to confine complex cleaning fluids, able to remove aged varnishes. These complex fluids are 5-component water-based nanostructured systems, where organic solvents are partially dispersed as nanosized droplets in a continuous aqueous phase, using surfactants. The rheological behavior of the SIPN and the nanostructure of the fluids loaded into the gel were investigated, and the mechanical behavior of the gel was optimized by varying both the cross-linking density and the polymer concentration. Once loaded with the complex fluids, the hydrogels maintained their structural and mechanical features, while the complex fluids showed a decrease in the size of the dispersed solvent droplets. Two challenging case studies have been selected to evaluate the applicability of the SIPN hydrogels loaded with the complex fluids. The first case study concerns the removal of a surface layer composed by an aged brown resinous patina from a wood panel, the second case study concerns the removal of a homogeneous layer of yellowed varnish from a watercolor on paper. The results show that the confinement of complex fluids into gels allowed unprecedented removal of varnishes from artifacts overcoming the limitations of traditional cleaning methods.

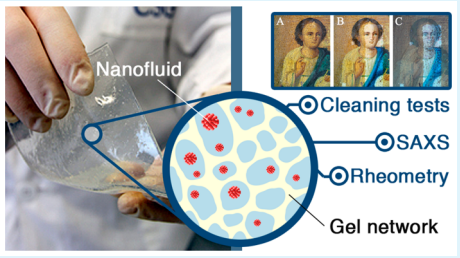

KEYWORDS: *chemical hydrogels, semi-interpenetrated polymer networks, SAXS, rheology, cleaning, varnish removal, watercolor*

1. INTRODUCTION

Easel paintings often exhibit surface coatings meant to prevent damage, repair, or enhance the visual appearance of the artifacts. However, the natural aging of these materials may lead to discoloration (yellowing), which alters the original appearance of paintings.[1,2] Hence, the removal of aged varnishes and coatings using organic solvents is one of the most common procedures in painting conservation. However, this involves several drawbacks, such as the toxicity of solvents, the risk of swelling or leaching original components (dyes, pigments' binders), and the redeposition of solubilized coatings within the pores of the artifact.[3,4]

Complex fluids (mainly micellar systems and microemulsions) have been proven as a valid alternative for the cleaning of works of art, owing to their low toxicity and enhanced effectiveness as opposed to neat organic solvents.[5−7] For instance, water-based fluids were shown to be highly efficient in the swelling, solubilization and removal of several different hydrophobic coatings.[8−13] However, despite their versatility shown by different case-studies,[14] the use of these aqueous fluids on water-sensitive substrates (canvas, paper, and some organic binders) might cause mechanical stress, swelling, and detachment of the paint layer.[15]

To overcome this issue and retain the advantages of using water-based fluids, we investigated the confinement of micellar and microemulsion systems into matrices, so as to achieve the gradual release of the fluids onto the painting surface, and control the cleaning action. Traditional confining systems adopted by restorers include thickeners (e.g., poly(acrylic acid) and cellulose ethers[16,17]), and polysaccharide gels[18−20] (e.g., agar−agar and gellan gum), where the confining network is made of polymer chains interacting through noncovalent forces. However, some of these materials are prone to leave residues on the painting surface. Moreover, the control of the cleaning action is poor, as fluid retention is typically inadequate for application on highly sensitive substrates such as hydrophilic fibers, soluble inks, or dyes. Alternatively, in the past few years we have been proposing highly viscous polymer dispersions[21−25] and chemical gels[26−28] that allow controlled cleaning

Received: January 31, 2018
Accepted: May 4, 2018
Published: May 4, 2018

DOI: 10.1021/acsami.8b01841
ACS Appl. Mater. Interfaces 2018, 10, 19162−19172

without leaving detectable dispersion/gel residues. In particular, the use of hydrogels based on semi-interpenetrated polymer networks (SIPNs) is advantageous because both the hydrophilicity and porosity of the gels can be tuned to optimize the swelling response and the liquid release kinetics.[29] SIPNs formed by the cross-linking polymerization of 2-hydroxyethyl methacrylate/*N*,*N*′-methylenebis(acrylamide) (HEMA/MBA) in the presence of linear PVP, are hydrogels effective in the removal of hydrosoluble dirt from water-sensitive surfaces.[30−32]

In this work, we present the combination of pHEMA/PVP-based SIPN hydrogels loaded with swollen micellar systems/microemulsions, hereafter, named "complex fluids", which, to the best of our knowledge, represents the most advanced wet-cleaning technology for the removal of hydrophobic materials from water-sensitive artifacts. The properties of the combined SIPN/complex fluid systems are here characterized thoroughly. A rheological study was carried out to optimize the elasticity of the SIPN hydrogels by varying their composition. Both water-loaded and complex fluid-loaded hydrogels were investigated by means of rheology and small angle X-ray scattering (SAXS), accounting for possible changes in the gel or in the complex fluid structure. Two complex fluids were selected for confinement in the pHEMA/PVP hydrogels. The first one, named EAPC,[14] is a water-based five-component system, containing sodium dodecyl sulfate (SDS), 1-pentanol (PeOH), propylene carbonate (PC), and ethyl acetate (EA). EAPC is a highly effective and versatile cleaning fluid, originally developed for the removal of synthetic polymer coatings from wall paintings.[8,9,14] The second system, named MEB, was specifically developed for this investigation. It includes *N*,*N*-dimethyldodecan-1-amine oxide (DDAO) as the surfactant, and a 1:1:1 (w/w/w) mixture of 2-butanone (methyl ethyl ketone, MEK), EA, and butyl acetate (BuA). Both, MEK and EA are effective solvents for the swelling and solubilization of several polymeric coatings. The presence of BuA, a slightly less polar molecule than MEK and EA, extends the range of materials that can be swollen or removed by the MEB cleaning system. Amine oxides are nonionic/zwitterionic surfactants widely used in detergency, cosmetics and toiletry, and drug delivery.[33,34] They show high dispersing power toward several water-insoluble organic substances, are dermatologically safe and easily biodegraded by aerobic microorganisms.[34] These features are particularly relevant because they guarantee low toxicity and high eco-compatibility to DDAO-based cleaning systems. Moreover, in acidic conditions DDAO becomes cationic, and even around neutrality it is slightly protonated (2−20%).[35−37] As a consequence, in mild pH conditions DDAO does not show a cloud point[38,39] and can be safely used when temperature-sensitive formulations cannot be employed (e.g., systems containing nonionic alkyl polyglycolether surfactants).

The efficacy of the new SIPN/complex fluid cleaning systems was assessed on real case studies, where the selective removal of aged surface varnishes from an easel painting and a drawing on paper was achieved, opening new perspectives in the conservation of water-sensitive artifacts.

2. MATERIALS AND METHODS

2-Hydroxyethyl methacrylate (HEMA; Sigma-Aldrich, assay 97%), poly(vinylpyrrolidone) (PVP; Sigma-Aldrich, average $M_w \approx 1.3 \times 10^6$ Da), ammonium persulfate (APS; Sigma-Aldrich, assay 98%), 2,2-azobis(2-methylpropionitrile) (AIBN; Fluka, assay 98%), *N*,*N*-methylene-bis(acrylamide) (MBA; Fluka, assay 99%), *N*,*N*,*N*′,*N*′-tetramethylethylenediamine (TEMED; Fluka, assay ≥99%), sodium dodecyl sulfate (SDS; Sigma-Aldrich, assay >98%), 1-pentanol (PeOH; Merck, assay ≥98.5%), ethyl acetate (EA; Sigma-Aldrich, ACS reagents, assay ≥99.5%), propylene carbonate (PC; Sigma-Aldrich, assay 99%), *N*,*N*-dimethyldodecan-1-amine oxide (DDAO; Sigma-Aldrich, 30% (w/w) aqueous solution), 2-butanone (MEK; Sigma-Aldrich, assay 99%), and butyl acetate (BuA; Sigma-Aldrich, assay ≥99%) were used as received. AIBN was recrystallized twice from methanol prior to use. Water was purified by a Millipore MilliRO-6 Milli-Q gradient system (resistivity > 18 MΩ cm).

2.1. Preparation of SIPNs and Loading with Complex Fluids. For the SIPNs synthesis, 2-hydroxyethyl methacrylate (HEMA) monomer and the cross-linker *N*,*N*′-methylenebis(acrylamide) (MBA) were added to a water solution containing polyvinylpyrrolidone (PVP) (average $M_w \approx 1.3 \times 10^6$ Da). The reaction mixture was bubbled with nitrogen for 5 min to remove oxygen, and then radical initiator 2,2′-Azobis(2-methylpropionitrile) (AIBN) was added in a 1:0.01 monomer/initiator molar ratio. The reaction mixture was gently sonicated for 30 min in pulsed mode, and then casted to molds and placed at 60 °C for 4 h. After polymerization, the hydrogels were placed in containers with distilled water in order to eliminate nonreacted HEMA (the yield of the polymerization reaction is almost 93%). The water was renewed twice a day, for 7 days. Table SI1 reports the composition (w/w %) of the starting mixture (before polymerization) for the hydrogels. The final gel composition after washing was determined as described in the Supporting Information, and are reported in Tables SI2 and SI3. The gels were shaped as flat sheets (2 mm thickness).

The complex fluids EAPC (73.3% H_2O, 3.7% SDS, 7% PeOH, 8% EA, 8% PC) or MEB (81.9% H_2O, 6.1% *N*,*N*-DDAO, 4% MEK, 4% EA, 4% BuA) were loaded into SIPNs by gel immersion for at least 12 h prior to use. All the measurements and application tests were carried out by means of fully hydrated gels if not otherwise indicated.

2.2. Rheology Measurements. The viscoelastic features of hydrogel sheets were studied with a DHR rheometer from TA Instruments equipped with a parallel plate geometry of 40 mm diameter. All hydrogel samples where cut to fit the plate shape under a trim gap and then equilibrated for 20 min at 25.00 ± 0.01 °C (Peltier temperature control system). The plate was lowered to the measuring position in the *z*-axis force controlled mode; the maximum squeezing force was 0.7 N. This was inspected during a series of rheology measurements on the same sample over time. The rheological behavior was determined by measuring the storage, G', and the loss, G'' moduli in an oscillation regime in the linear viscoelastic region of deformations (amplitude sweep shown in Figure SI2). G' and G'' were measured over the frequency range 10^2-10^{-3} Hz at a temperature of 25.00 ± 0.01 °C, with a strain of 0.1%. The values of the stress amplitude were confirmed through amplitude sweep runs to ensure that all measurements were performed within the linear viscoelastic region.

The plate−plate gap was set up as a function of the thickness of the gels to maintain the normal force constantly equal to 0.5 N.

2.3. Small-Angle X-ray Scattering. SAXS measurements were carried out with a HECUS S3-MICRO camera (Kratky-type) equipped with a position-sensitive detector (OED 50M) containing 1024 channels of width 54 μm. Cu Kα radiation of wavelength λ = 1.542 Å was provided by an ultrabrilliant point microfocus X-ray source (GENIX-Fox 3D, Xenocs, Grenoble), operating at a maximum power of 50 W (50 kV and 1 mA). The sample-to-detector distance was 281 mm. The volume between the sample and the detector was kept under vacuum during the measurements to minimize scattering from the air. The Kratky camera was calibrated in the small angle region using silver behenate (d = 58.38 Å).[40] Scattering curves were obtained in the q-range between 0.01 and 0.54 Å^{-1}, assuming that q is the scattering vector ($q = 4\pi/\lambda \sin\theta$), and 2θ the scattering angle. Hydrogel samples were placed into a 1 mm thick demountable cell having Nalophan films as windows, while liquid samples were put in 2 mm thick quartz capillary tubes sealed with hot-melting glue. The temperature was set to 25 °C and was controlled by a Peltier element, with an accuracy of 0.1 °C. All scattering curves were corrected for the empty cell contribution considering the relative transmission factor.

DOI: 10.1021/acsami.8b01841
ACS Appl. Mater. Interfaces 2018, 10, 19162−19172

For detailed information on the fitting models adopted in this study, please refer to the Supporting Information.

Short SAXS measurements (1−2 min) were performed to check any X-ray radiation damage to the hydrogel structures during the acquisition. No change in the final SAXS curve was evidenced confirming that the radiation damage was negligible in the conditions reported for this type of experiment.

2.4. FTIR. A FTIR spectrometer (Thermo Nicolet Nexus 870) in attenuated total reflectance FT-infrared mode (ATR-FTIR), equipped with a Golden Gate diamond cell, was used to investigate the presence of possible gel residues on the surface of easel paintings after the cleaning treatments. Data were collected with an MCT detector. The spectra were obtained from 128 scans with a 4 cm^{-1} spectral resolution, in the 4000−650 cm^{-1} range.

2.5. Scanning Electron Microscopy. A FEG-SEM ΣIGMA (Carl Zeiss, Germany) was used to acquire images from xerogels (freeze-dried hydrogels) using an acceleration potential of 1 kV and a working distance of 1.4 mm.

2.6. Removal of Hydrophobic Materials Using Complex Fluid-Loaded SIPNs. Two case studies (early 20th century artworks) were used to confirm the efficiency of SIPNs loaded either with the EAPC or MEB complex fluid: (i) a "varnish-based" panel painting where two different types of varnishes were used (one as a binder for pigments, and the other as a top finishing layer) and (ii) a varnished watercolor on paper. The sheets of hydrogels, loaded with the complex fluids, were used directly on the surface of the paintings. The application (1−2 min) resulted in the swelling of the unwanted varnish layers, which were then easily removed by gentle mechanical action using a slightly wet cotton swab.

Further information on the methods and materials used in the present paper are reported in the Supporting Information.

3. RESULTS AND DISCUSSION

The physicochemical properties of chemical gels can be tuned by interpenetrating a linear polymer in the hydrogel network, and by changing the nature and the concentration of such linear polymer. Thus, a SIPN is an ideal system to control properties such as hydrophilicity, stickiness or elasticity, while retaining the starting covalent network. The linear hydrophilic polymer PVP conveys a higher water retention capability to the original pHEMA network. Previous investigations by our group,[30] demonstrated that the optimal systems in terms of water retention and cleaning efficacy contain 10%−25% (w/w) of the chemical network (pHEMA/MBA), 25% of PVP, and 50−65% of water.

3.1. Rheology and Mechanical Behavior. The dynamic mechanical properties of two different series of pHEMA/PVP SIPNs (see Tables SI2 and SI3) were investigated by frequency sweep oscillation tests to obtain information on the role of HEMA and MBA, respectively the monomer and the cross-linker, and on the mechanical properties of the hydrogels, which are of paramount importance for application on artifacts. Figure SI3 shows the trend of the storage modulus G' and the loss modulus G'' at a constant strain of 5% as a function of the frequency, for the HEMA5−HEMA20 hydrogels (HEMA concentration increasing from HEMA5 to HEMA20). For all investigated samples, the storage modulus is always larger than the loss modulus, and no crossover between the G' and G'' curves is observed within the accessible range of frequency. This behavior is typical of solid-like fluids with infinite relaxation time, and accounts for the chemical nature of the cross-links (covalent bonds) in the pHEMA network. Furthermore, G' is almost independent of the frequency of the applied stress, and changes from about 720 to 19 500 Pa increasing the concentration of HEMA. In this case, G' is proportional to the entanglement density[41,42] (i.e., polymer network concentration), while the rheological behavior remains almost unchanged. The dependence of G' on the polymer weight fraction ϕ is largely discussed in the literature.[43] In most cases, the trend is described by a power law function, $G' \propto \phi^n$.[44] Figure 1 shows the variation of the G' values at ω = 1 Hz for

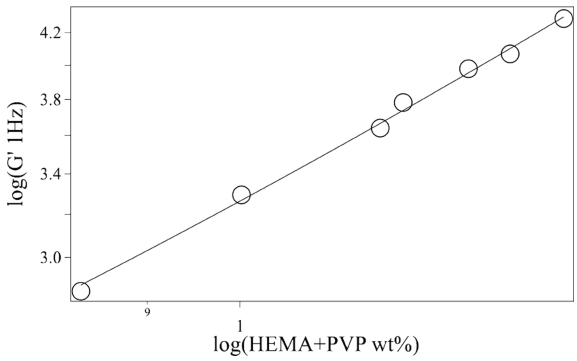

Figure 1. Double-logarithmic scale representation describing the effect of the concentration of HEMA/PVP network on the value of the elastic modulus G' at 1 Hz. The line represents the best fitting (log G'(1 Hz) = 2.36 log (wt % HEMA+PVP) + 0.90 (R^2 = 0.99601)).

pHEMA/PVP hydrogels as a function of the total wt % of pHEMA/PVP network. The power-law fit of the experimental data results in a n value of 2.36 ± 0.08. According to the theory describing the behavior of polymers in solution, this value suggests that the expansion of the pHEMA network occurs through a percolation mechanism.[45] This involves first the formation of clusters composed by pHEMA oligomers and then their connection through the whole volume of the sample with the formation of an infinite 3D covalent network. This model, which relies upon a critical phenomenon of connectivity, has been applied to the formation of chemically cross-linked networks.[44]

Figure 2 shows the trend of the elastic modulus, G' (at ω= 1 Hz), as a function of the MBA concentration, while maintaining

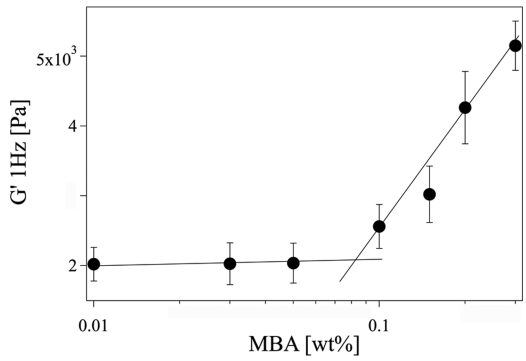

Figure 2. Semilog plot of the G' (obtained at 1 Hz) dependence on cross-linker concentration (MBA).

the amount of HEMA and PVP constant at 10.5% (w/w) and 24.3%, respectively (see Table SI3). As it is clear from the figure, a critical value of the MBA concentration (~0.08%) exists, above which a drastic increase of G' (1 Hz) occurs. This behavior can be attributed to the progressive formation of a percolated 3D polymer network induced by the chemical connection of pHEMA clusters. From a practical point of view, SIPNs with MBA concentration below 0.08% can be easily

DOI: 10.1021/acsami.8b01841
ACS Appl. Mater. Interfaces 2018, 10, 19162−19172

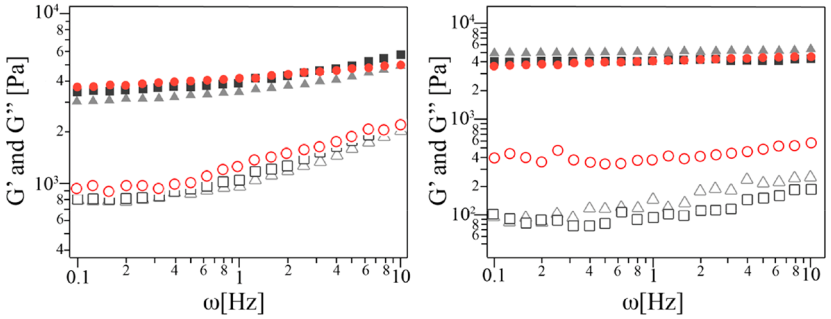

Figure 3. Storage G' (filled marks) and loss G'' (empty marks) moduli for (left) HEMA16.8 and (right) HEMA10.5 hydrogels (Table SI4) loaded with different fluids: water (red circles), EAPC (gray squares), MEB (gray triangles).

squeezed while above this threshold the system becomes more rigid.

The effect of loading EAPC and MEB complex fluids into the SIPNs was also investigated to determine whether the inclusion of the fluids affects the gel's rheological properties. The investigation was carried out on two gel formulations (named "HEMA 10.5" and "HEMA 16.8", whose composition is shown in Table SI4) that were selected as they exhibit high water retention, thus they are expected to grant optimal control when removing varnishes from the paintings. The profile of the frequency sweep curves, collected for SIPNs loaded with water or complex fluids, shows no substantial differences, that is, the viscoelastic behavior is not affected by replacing water with EAPC or MEB (see Figure 3A and B).

These gels behave as sponges capable of absorbing different complex nanostructured fluids without any meaningful change in their mechanical properties. This is in agreement with the FEG-SEM investigation of xerogels obtained by freeze-drying HEMA10.5 SIPNs loaded either with water or with the fluids: no differences were noticed in the porous structure at the microscale (an image of the porous network of the hydrogel is shown in Figure 4). The xerogels display a broad pore size distribution with diameters ranging from 5 to 39 μm.[30]

3.2. SAXS Investigation. SAXS measurements were performed to investigate possible changes in the nanostructure of the two complex fluids (i.e., EAPC and MEB) upon loading into SIPN hydrogels. Figure 5 shows the SAXS intensity distribution of the HEMA16.8 SIPN loaded with EAPC (top panel) and MEB (bottom panel), in comparison with that of the pure systems. In both cases, the curve of the gel/complex fluid system is a combination of the scattering contributions of the separate gel and complex fluid systems.

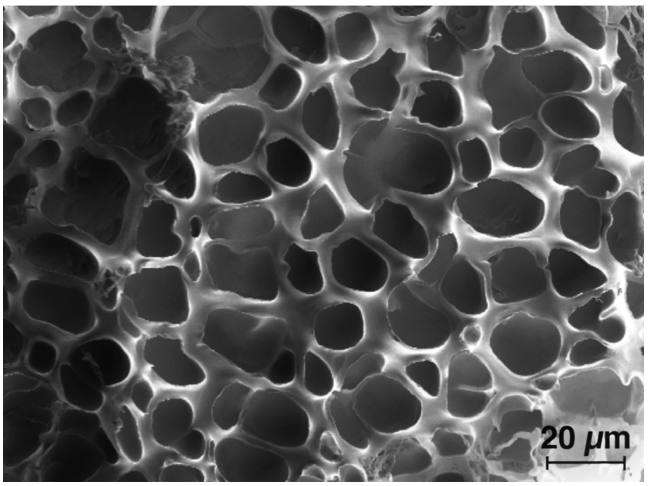

Figure 4. FEG-SEM image of the xerogel obtained by freeze-drying a HEMA10.5 SIPN loaded with water. No difference in the porous structure is observed for xerogels obtained from SIPNs loaded with the EAPC or MEB nanostructured fluids.

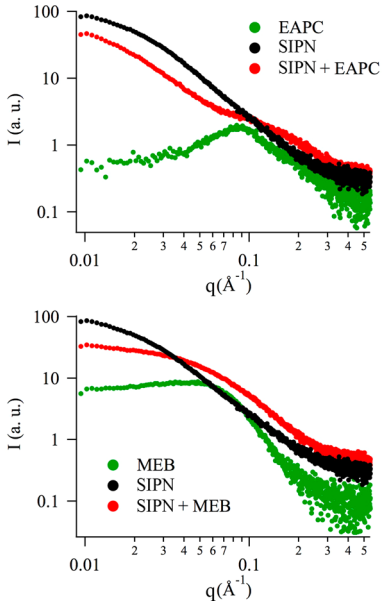

Figure 5. Scattering curves for (top) water-loaded SIPN, neat EAPC, EAPC⊂SIPN combined system and (bottom) water-loaded SIPN, neat MEB, MEB⊂SIPN combined system.

Two assumptions were made for the data fitting. (i) The scattering intensities coming from the PVP solution, constituting the "continuum" of the hydrogel matrix, and from the complex fluid are considered purely additive signals independent of each other (see Supporting Information file for further details); this is justified by the good match between the scattering profile of neat EAPC and that obtained by subtracting the signal of a PVP solution (opportunely scaled) from the combined (PVP solution + EAPC) system (see Figure SI5, where the subtraction curve is named $EAPC_{PVP}$), in agreement with the fact that the complex fluid does not interact with the linear polymer interpenetrating the hydrogel (PVP). (ii) The gel structure does not dramatically change after loading the complex fluids, which is justified by the rheological analysis and FEG-SEM investigation discussed in the previous section.

DOI: 10.1021/acsami.8b01841
ACS Appl. Mater. Interfaces 2018, 10, 19162−19172

According to these assumptions, the scattering signal of the pure hydrogel was opportunely scaled for the relative transmission factor and subtracted from the curve measured on the correspondent gel + complex fluid system. The differences observed after the subtraction can be associated with the interaction between the complex fluid and the chemical skeleton of the hydrogel. The resulting curves can be interpreted as the signal coming from the complex fluid confined inside the gel (hereafter, respectively, $EAPC_{gel}$ and MEB_{gel}). The comparison of $EAPC_{gel}$ and MEB_{gel} with the scattering profiles of the two neat complex fluids, suggests that slight changes occurred in the fluids' nanostructure (see Figure 6, high q region).

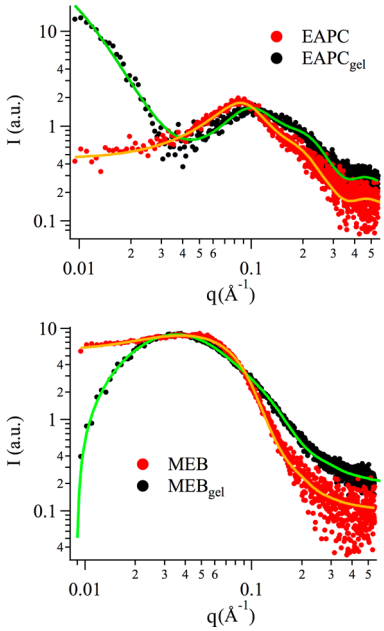

Figure 6. (top) SAXS scattering profiles of EAPC and $EAPC_{gel}$. (bottom) SAXS scattering profiles of MEB and MEB_{gel}. Continuous lines represent best fits of the experimental data.

In the following paragraphs the effect of the loading of the two complex fluids is discussed separately.

3.2.1. EAPC-Loaded SIPN. EAPC was extensively studied during the last years, mainly by small angle neutron contrast variation, and detailed information about its nanostructure are available in the literature.[8,46,47] Essentially, in EAPC the propylene carbonate is partitioned between the continuous water phase and the dispersed micelles formed by the surfactant (SDS), the cosurfactant (PeOH), and ethyl acetate. In this Research Article, the SAXS curve of the neat complex fluid was modeled using a core−shell prolate ellipsoids form factor, while the interaction potential between the scattering objects was implemented according to a screened Coulomb potential within NAR-MMSA (nonadditive radius multicomponent mean sphere approximation).[48−51] The total scattered intensity, $I(q)$, is given by the following equation:[50,52]

$$I(q) = N_p V_p^2 \Delta\rho^2 P(q) S(q) + bkg \quad (1)$$

where N_p is the number density of the scattering objects (cm^{-3}), V_p is the their volume (cm^3), $\Delta\rho$ is the contrast term (cm^{-2}), $P(q)$ and $S(q)$ are, respectively, the form factor and the structure factor, described more in detail in the Supporting Information.

The fitting results (see Table 1) are in good agreement with previous findings.[47] Some slight differences are observed with respect to published data, that is, the SDS micelles in this case are somewhat more globular. This can be ascribed to the different amount of impurities (i.e., mostly dodecanol) present in the SDS used in the present work, with respect to the surfactant batch used in the cited paper.[47] It is well described in the literature that *n*-alcohols (either short, medium, and long chain) have an impact on the aggregation behavior of SDS and especially on the aggregation number and aggregates' shape at the equilibrium.[53]

Table 1. Fitting Parameters Obtained for EAPC and $EAPC_{gel}$[a]

fitting parameter	EAPC	$EAPC_{gel}$	SIPN[b]
ϕ	0.19 ± 0.1	0.18 ± 0.1	
a (Å)	61.5 ± 3.2	41.1 ± 3.2	
b (Å)	12.7 ± 0.5	12.1 ± 0.1	
t (Å)	2.5 ± 0.1[c]	5.6 ± 0.1[c]	
Z (1.60×10^{-19} C)	8.0 ± 1.7	7.6 ± 0.8	
I_0 (a.u.)		70.0 ± 3.6	45.3 ± 2.5
k (Å)		104.0 ± 4.9	36 ± 3.2

[a] ϕ is the volume fraction of the micellar phase, a is the major semi-axis of the ellipsoidal micelle core, b is the minor semi-axis of the ellipsoidal micelle core, t is the shell thickness, Z is the net charge of each micelle. [b] Data in agreement with ref 30. [c] The shell has only partial meaning because its value is close to the resolution of the experiment.

Figure 6 (top) shows that, while the scattering profiles of EAPC and $EAPC_{gel}$ are very similar in the medium/high-q region, for low q values the two curves significantly diverge. In particular, the scattering intensity of $EAPC_{gel}$ presents an excess scattering at low q. This can be attributed either to a change in the gel nanostructure, to clustering of the micellar system onto the polymer network of the SIPN, or to a combination of these two effects. To take into account this experimental evidence, an extra term in the fitting model was considered.

In previous works,[30] these gels (loaded with water) were modeled using the Debye−Bueche approach, where the SAXS intensity distribution is considered as the sum of two q-dependent contributions. The first term is a Lorentzian function that accounts for the scattering associated with a tridimensional network with a characteristic mesh (or blob) size (2.8 nm, in the case of HEMA16.8[30]). The second contribution is related to the scattering at low q produced by inhomogeneities, such as solid-like polymer domains (3.6 nm, in the case of HEMA16.8, see Table 1). In the present study, we adopted a phenomenological approach considering the excess scattering as a result of a new inhomogeneity generated by the gel-complex fluid interaction. Concurrently, we implicitly assumed that the mesh size of the chemical network is not affected by this interaction. Therefore, eq 1 was modified adding an explicit term to account for this extra contribution:

$$I(q) = N_p V_p^2 \Delta\rho^2 P(q) S(q) + \frac{I_o}{(1 + q^2 k^2)^2} + bkg \quad (2)$$

where I_0 is the excess intensity at zero q, and k is the average dimension of the inhomogeneity domains accessible with SAXS measurements. The fitting was then performed using eq 2, and a good fitting curve for the whole q range investigated was

DOI: 10.1021/acsami.8b01841
ACS Appl. Mater. Interfaces 2018, 10, 19162−19172

obtained (see Figure 6-top, green line). From the comparison of the parameters obtained from the fitting of the two curves (see Table 1), it is evident that once EAPC is confined in the gel, the main effect observed is a small decrease in the overall micellar size, while neither the volume fraction nor micellar charge change significantly (Table 1). Hence, it is likely that the nanostructure of EAPC is preserved when it is loaded into the gel. *This is of crucial importance from an applicative standpoint: the cleaning efficacy of the complex fluid confined in the hydrogel is expected to be comparable with that of the free EAPC.*

The average size of the inhomogeneity is increased up to about 10 nm after loading the complex fluid into the gel (see Table 1). We attributed this effect to a "micro-phase separation" of pHEMA, surfactant and PVP, which generates a solid-like region (see Figure 7). Interestingly, this region has a similar size to EAPC micelles (see Table 1).

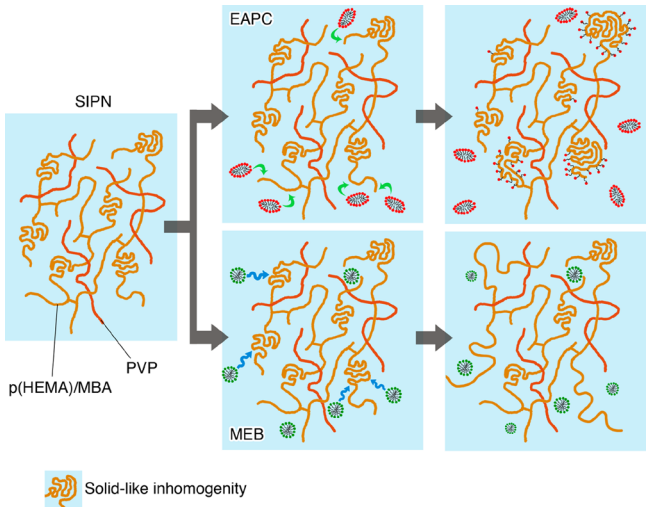

Figure 7. Cartoon illustrating the hypothesized interaction of the two complex fluids with the hydrogel, according to SAXS data interpretation. In the case of EAPC, the average size of the inhomogeneities increases of about 10 nm after the loading of the complex fluid into the gel, due to a "micro-phase separation" of pHEMA, surfactant and PVP, which generates a solid-like region. In the case of MEB, conversely, the solvents contained in the micelles promote the disentanglement of pHEMA inhomogeneities.

3.2.2. MEB-Loaded SIPN. Differently from EAPC, the MEB system was not studied in previous works. MEB is a complex five-components system, thus the fitting of the SAXS profile is not trivial owing to the presence of several interdependent variables. As already reported, DDAO holds low surface charge when associated in micelles[35−37,54] even if its nature is either nonionic or zwitterionic. A good fitting curve (see Figure 6-bottom, yellow line) was obtained modeling the system as composed by polydisperse core−shell spherical particles with low surface charge. The fitting parameters for MEB are reported in Table 2.

As for EAPC,[47] the MEB complex fluid only partly fits the classical definition of a microemulsion. In fact, both systems contain supramolecular aggregates formed by the interaction of surfactants and solvents, but there is not a well-defined oil phase clearly separated by the aqueous bulk phase by a surfactant/cosurfactant layer. Instead, the solvents are partly dissolved in water and partly included in the micellar phase, where they can be located either in the hydrophobic core or in the polar shell, according to their polarity. As in the case of similar complex fluids,[12,47,55] also for MEB the fitting results show that 40% of EA and 70% of MEK are adsorbed at the droplets interface together with the total amount of butyl acetate. Moreover, the overall micellar size is in agreement with the length of fully extended DDAO molecules, so that the presence of oil in the core is excluded, while the micelle is swollen by the inclusion of polar cosolvents at the interface of the nanodroplets.

Table 2. Fitting Parameters Obtained for MEB and MEB_{gel} Scattering Profiles[a]

fitting parameter	MEB	MEB_{gel}
ϕ	0.15 ± 0.1	0.13 ± 0.1
r (Å)	24.2 ± 2.2	11.5 ± 3.0
t (Å)	1.5 ± 0.1[b]	1.6 ± 0.5[b]
Poly (0,1)	0.4 ± 0.1	0.8 ± 0.1
Z (1.60×10^{-19} C)	3.9 ± 0.4	2.6 ± 2.5
I_0 (a.u.)		- 15.6 ± 4.8
k (Å)		35.0 ± 2.1

[a]ϕ is the volume fraction of the micellar phase, r is the radius of the micelle core, t is the shell thickness, *Poly* is the polydispersity index of the micelles' core, and Z is the net charge of each micelle. [b]The shell has only partial meaning because its value is close to the resolution of the experiment.

Micellar charge is low, though slightly higher than expected,[54] probably due to the presence of polar solvents in the shell region, which alter both the usual ionization degree of DDAO and the dielectric constant of the environment. Finally, core polydispersity is 0.4, which is high, nonetheless reasonable for a complex fluid.

When looking at the MEB_{gel} (the MEB confined into the gel) scattering profile, similarly to what observed for EAPC, we can notice that, while the complex fluid does not seem to be significantly altered by its confinement in the gel, in the low-q region MEB_{gel} and MEB curves significantly differ. In this case, a scattering intensity decrease is observed at low q values. Using a symmetric approach to the one used for EAPC, from eq 2 a negative I_0 was expected; the fitting results are reported in Table 2.

We could hypothesize that MEB complex fluid interacts with the gel causing the disappearance of part of the solid-like inhomogeneities. This suggests that some solvents included in the complex fluid cloud locally swell the polymeric domains causing pHEMA chains to partially disentangle (see Figure 7). This hypothesis could be confirmed by SANS contrast matching experiments. This effect has no consequences in the profile of the frequency sweep reported in Figure 3 because the entity of the changes are too limited to be detected through rheological measurements.

As in the case of EAPC, the nanostructure of the MEB complex fluid is preserved inside the gel, while micelles get smaller and the volume fraction is slightly decreased. This is also in agreement with the hypothesis of some solvent migrating from the complex fluid to the polymeric network of the gel, with subsequent local swelling and softening of pHEMA solid-like domains. Micellar charge does not change significantly, while some concerns arise from 0.8 core polydispersity that has poor physical significance. Most likely this parameter accounts for all the uncertainties and approximations of the fitting approach that was adopted. However, the high polydispersity might indicate that not all the

DOI: 10.1021/acsami.8b01841
ACS Appl. Mater. Interfaces 2018, 10, 19162−19172

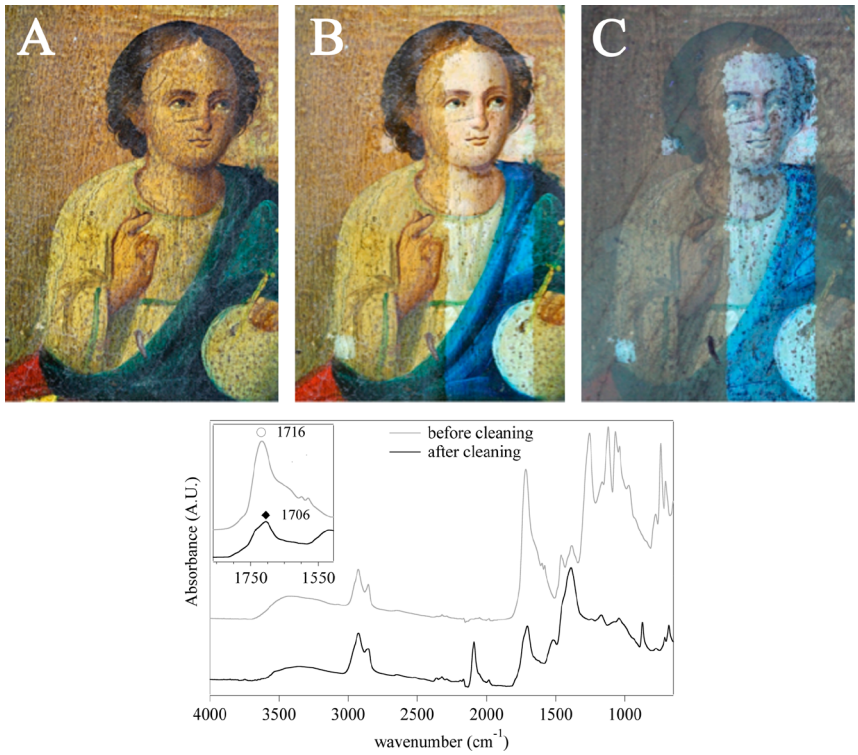

Figure 8. Visible light image showing a detail of the Icon (panel painting), before (A) and after (B, visible light; C, UV light) the cleaning by means of the EAPC-loaded SIPN. The images of the icon are printed with the kind permission of Aurelia Chevalier. Bottom: ATR-FTIR spectra of Icon (panel painting) surface before and after cleaning. The inset highlights the bands assigned to the carbonyl stretching vibration of the undesired brownish varnish (1716 cm^{-1}) and of the paint binder (1706 and 1735 cm^{-1}).

micelles get smaller, rather a coexistence of smaller and bigger aggregates, which contribute to the high polydispersity index, is present.

The value of the parameter k shows that the average size of inhomogeneous domains disappearing after gel-complex fluid interaction is about 3.5 nm. Most interestingly, entangled polymer domains in the HEMA16.8 formulations are about 3.6 nm,[30] which perfectly fits the hypothesis about disentanglement of pHEMA chains that occurs as a result of the complex fluid loading. Moreover, by comparing I_0 of the neat gel and of MEB_{gel}, it is possible to assume that about 1/3 of the solid-like domains disappear.

Finally, although the two complex fluids interestingly showed opposite behaviors when interacting with pHEMA/PVP networks, in both cases their nanostructure is left almost unaltered by confinement in the hydrogel. This is a remarkable finding in view of predicting the effectiveness of the combined systems in cleaning applications.

4. CASE STUDIES

Two case studies have been selected to evaluate the applicability of the SIPN hydrogels loaded with the complex fluids. The first case study concerns the removal of a surface layer composed by an aged brown resinous patina from a wood panel representing the Virgin with the Child. *This case is representative of challenging interventions, where a selective and controlled cleaning process is necessary to avoid the diffusion of the fluids into the pictorial layer, which could result in the swelling of the paint binder.* The second case study concerns the removal of a homogeneous layer of a yellowed varnish from a watercolor on paper. *The controlled delivery of the complex cleaning fluid is necessary to remove the varnish without leaching water-sensitive pigments or swelling the paper fibers.*

Therefore, both cases are optimal candidates for testing the efficiency of SIPN hydrogels loaded with complex fluids for the selective removal of unwanted surface layers, while preserving the physicochemical integrity of the original artistic layers.

Both HEMA10.5 and HEMA16.8 hydrogels (loaded with EAPC and MEB) were selected for preliminary tests, but the latter gel proved to be the most suitable in both case studies, owing to the particularly water-sensitive character of the artifacts that required highly retentive confining systems.

For the cleaning of the wood panel, the hydrogel loaded with EAPC system gave the best results. The cleaning procedure consisted in applying the hydrogel sheet (0.5 × 1 cm^2, 2 mm thick) for 1 min, and then gently and selectively removing the swollen resin with a cotton swab (Figure SI6). In Figure 8, the overall result of cleaning with a gel loaded with EAPC is shown (under Vis and UV light).

A further examination of the gel cleaning efficiency was carried out by means of ATR-FTIR (Figure 8-bottom). Natural varnishes commonly found as historic finishes of artworks usually include terpene-based resins (e.g., sandarac, mastic) and polyhydroxy acid–based resins (e.g., shellac), besides oils, waxes and polysaccharide gums.[56] One of the most characteristic IR bands is the carbonyl stretching vibration, which ranges from 1695 to 1715 cm^{-1} for terpene-based varnishes, or from 1715 to 1722 cm^{-1} for polyhydroxy acid–based coatings.[56] The spectrum collected on the painting surface before the cleaning intervention shows a strong band centered at 1716 cm^{-1} (C═O str.) and absorptions at ∼1650 (shoulder, C═C str.), 1461 (CH_2 bend.), 1382 (−C−H bend.), 1257 (C−O str., ester), 1165 (C−O str., acid), 1040 (C−O str., alcohol), 970 and 925

DOI: 10.1021/acsami.8b01841
ACS Appl. Mater. Interfaces 2018, 10, 19162−19172

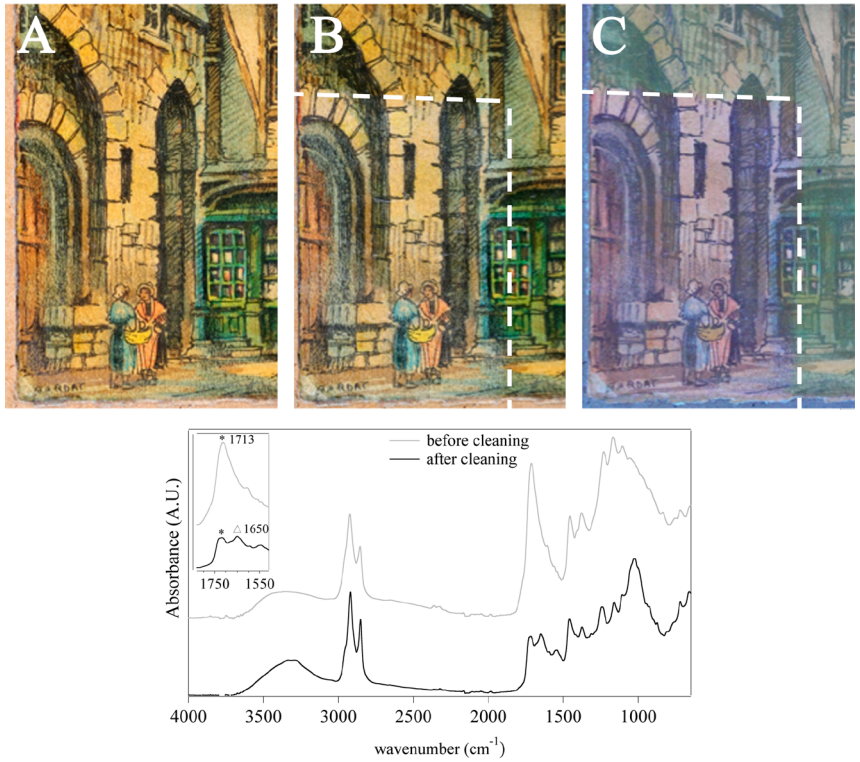

Figure 9. Detail of a watercolor on paper, before (A) and after the cleaning intervention (B, visible light; C, UV light). The UV fluorescence photograph (C) highlights the removal of the varnish (the cleaned area appears as bluish). The images of the watercolor are printed with the kind permission of Aurelia Chevalier. Bottom: ATR-FTIR spectra of the watercolor on paper before and after the cleaning intervention. The inset highlights the 1750−1550 cm^{-1} region, with the absorptions of the varnish layer (1713 cm^{-1}, C═O str.) and of the paper support (1650 cm^{-1}, OH bend. of water absorbed in cellulose fibers).

cm^{-1} (═C−H bend.), which suggest the presence of a polyhydroxy acid−based resin.[56] The spectrum of the painted surface after cleaning shows a band at 1706 cm^{-1} with a shoulder at ∼1735 cm^{-1}, while the band at 1716 cm^{-1} is no longer observable (see inset in Figure 8). The C═O stretching band at 1706 cm^{-1} and the absorptions at 1390, 1240, 1170, and 1041 cm^{-1}, suggest the presence of a terpene-based resin.[56] The shoulder at 1735 cm^{-1} (C═O str.), together with aliphatic C−H band at 715 cm^{-1} and the C−O absorptions at 1240 and 1169 cm^{-1} indicate the presence of an oil binder (e.g., linseed oil).[56] The bands at 874 and 712 cm^{-1} are due to the presence of $CaCO_3$ (CO_3 asymmetric and symmetric bending[57]), and the strong absorption at 2090 cm^{-1} (CN str.) is due to the Prussian blue pigment.

The ATR-FTIR analysis is in good agreement with the UV-fluorescence investigation, where the brownish UV fluorescence of the top layer (clearly observable in the non-cleaned areas) indicates the presence of aged shellac,[58] while the blueish fluorescence observable in the cleaned areas can be attributed to the presence of both aged terpene-based resin[59] and drying oils.[60] This is consistent with the hypothesis that below the top layer, composed by polyhydroxy acid-based resin, lies a painted layer where the pigments are bound by a mixture of a terpene-based resin (e.g., dammar) and linseed oil. In fact, since the 19th century, natural resins have been used as popular additions to oil binders. Therefore, *the use of the hydrogel allowed the gradual and controlled release of EAPC cleaning system, leading to the selective removal of the undesired top (brownish) resin layer without affecting the painted layers underneath.*

Varnish removal from the watercolor on paper was carried out by means of the SIPN loaded with MEB system. In fact, preliminary tests using unconfined fluids showed that both MEB and EAPC complex fluids are able to remove the varnish, but EAPC causes the partial solubilization of the original black ink. In both cases, it was fundamental to avoid the swelling of the water-sensitive paper fibers while maintaining the advantages involved in the use of water-based complex cleaning fluids, in terms of cleaning effectiveness and decreased eco-toxicological impact as compared to the traditional solvents used in the restoration practice. The hydrogel sheet (0.5 × 1 cm^2, 2 mm thick), loaded with MEB cleaning system, was applied on the artwork surface for 2 min. The swollen and softened varnish was removed with a gentle mechanical action using a cotton swab slightly soaked with MEB (see Figures SI7 and 9). Two short successive applications over the same area, rather than a single longer application, allowed a more gradual and controlled removal of the unwanted layer. The achieved controlled swelling allowed minimizing the mechanical action with the swab, avoiding damage to the watercolor, the ink and the paper fibers.

ATR-FTIR was carried out on the artwork surface before and after the cleaning intervention (Figure 9-bottom). The spectrum collected before the cleaning intervention shows a strong adsorption centered at 1713 cm^{-1} (C═O str.), and absorptions at ca. 1605 cm^{-1} (C═C str.), 1453 cm^{-1} (CH_2 bend.), 1376 cm^{-1} (−C-H bend.), 1229 cm^{-1} (C−O str., ester), 1167 cm^{-1} (C−O str., acid), 1105 cm^{-1} (C−O str., alcohol), and 926 cm^{-1} (═C−H bend.) suggesting the presence of a natural resin, probably a polyhydroxy acid.[56] This hypothesis is supported by the analysis of the artifact under UV light that shows a yellow-brownish fluorescence emitted by the varnish layer.

DOI: 10.1021/acsami.8b01841
ACS Appl. Mater. Interfaces 2018, 10, 19162−19172

In the spectrum collected after the cleaning intervention, the intensity of the bands attributed to the varnish is strongly decreased indicating the removal of the surface coating. At the same time, the absorptions of the cellulosic support (paper) are clearly observable at 1650 (OH bend. of absorbed water), 1242 (C−OH bend. out-of-plane), 1160 (C−Casymm. str., ring breathing), and 1027 cm^{-1} (C−O str. alcohol).[61]

5. CONCLUSIONS

Advanced cleaning systems, obtained by the combination of two complex fluids (EAPC and MEB) and retentive SIPN hydrogels, have been characterized from a mechanical, rheological and structural point of view. By correlating the storage module G' of different pHEMA/PVP SIPNs with their polymer weight fraction, we showed that the gels formation follows a power law, supporting that the process occurs through a percolation mechanism. Interestingly, the cross-linker was shown to increase significantly the mechanical properties of the gel when its concentration is raised above the critical value of 0.08%. Uploading complex fluids does not significantly alter the rheological properties of SIPNs. Besides the interest from a physicochemical standpoint, this observation has considerable importance in view of practical applications, since the inclusion of cleaning fluids should not change the optimal mechanical properties of the gels. This behavior was observed for different gel formulations and for two different complex fluids. According to these findings, it can be inferred that the SIPNs act as "sponges", able to load different aqueous cleaning fluids without being altered or dramatically altering the fluids' properties. However, a more detailed analysis of the interaction between SIPNs and complex fluids showed that some modifications occur, meaning that complex fluids and SIPNs are weakly interacting. In particular, while the tridimensional structure of the SIPN network and the micellar structure of complex fluids inside the gel porosity are preserved, it was shown that the droplets of both EAPC and MEB fluids get slightly smaller when loaded into the SIPN; moreover, some minor modification of the pHEMA-MBA/PVP network can be hypothesized at the nanoscale. Upon loading EAPC, the average size of structural inhomogeneities in the SIPN polymer network increases of about 10 nm, due to a "micro-phase separation" of pHEMA and surfactant, which generates bigger solid-like regions. Conversely, in the case of MEB, the solvents contained in the micelles promote the disentanglement of pHEMA inhomogeneities. The reason why a different behavior is observed for the two complex fluids is not straightforward. The surfactant is different in the two systems, and this likely plays a key role in the interaction mechanism. However, also the different solvents included in EAPC and MEB formulations may have a different specific affinity for pHEMA or PVP, resulting in the two different observed mechanisms.

The application of the combined gel + fluid systems led to the controlled and selective removal of aged varnishes from the surface of two artifacts with different substrates (wood panel and paper), without altering the original components of the works.

In conclusion, this work represents a step forward in the characterization of pHEMA/PVP SIPNs. These systems, neat or combined with complex fluids, represent one of the most advanced systems for the cleaning of works of art, and are relevant for different fields related to detergency and coatings. Besides the applicative aspects, this study is also relevant to the understanding of the physicochemical properties of multicomponent microheterogeneous complex systems.

■ ASSOCIATED CONTENT

Supporting Information

The Supporting Information is available free of charge on the ACS Publications website at DOI: 10.1021/acsami.8b01841.

Further information about rheology measurements, SAXS fitting, and cleaning tests (PDF)

■ AUTHOR INFORMATION

Corresponding Author

*E-mail: baglioni@csgi.unifi.it.

ORCID

Emiliano Carretti: 0000-0001-5140-3123
Emiliano Fratini: 0000-0001-7104-6530
Piero Baglioni: 0000-0003-1312-8700

Present Address

†Procter & Gamble, Temselaan 100, 1853, Strombeek-Bever, Belgium.

Author Contributions

The manuscript was written through contributions of all authors. All authors have given approval to the final version of the manuscript. Michele Baglioni and Joana A. L. Domingues contributed equally to this work.

Notes

‡No kinship exists between these authors.
The authors declare no competing financial interest.

■ ACKNOWLEDGMENTS

Thanks are due to Marco Coletti (TA Instruments), and to Aurelia Chevalier (for providing the paintings). Joana A. L. Domingues thanks FCT for a fellowship allowing her staying at CSGI. This project has received funding from the European Union's Horizon 2020 research and innovation programme under grant agreement No 646063.

■ REFERENCES

(1) De la Rie, E. R. Old Master Paintings: A Study of the Varnish Problem. *Anal. Chem.* **1989**, *61* (21), 1228A−1240A.

(2) Chelazzi, D.; Chevalier, A.; Pizzorusso, G.; Giorgi, R.; Menu, M.; Baglioni, P. Characterization and degradation of poly(vinyl acetate)-based adhesives for canvas paintings. *Polym. Degrad. Stab.* **2014**, *107*, 314−320.

(3) Stolow, N. Application of Science to Cleaning Methods: Solvent Action Studies on Pigmented and Unpigmented Linseed Oil Films. In *Recent Advances in Conservation*; Butterworths: London, 1963; pp 84−88.

(4) Phenix, A.; Sutherland, K. The Cleaning of Paintings: Effects of Organic Solvents on Oil Paint Films. *Stud. Conserv.* **2001**, *46*, 47−60.

(5) Carretti, E.; Dei, L.; Baglioni, P. Solubilization of Acrylic and Vinyl Polymers in Nanocontainer Solutions. Application of Microemulsions and Micelles to Cultural Heritage Conservation. *Langmuir* **2003**, *19* (19), 7867−7872.

(6) Carretti, E.; Giorgi, R.; Berti, D.; Baglioni, P. Oil-in-Water Nanocontainers as Low Environmental Impact Cleaning Tools for Works of Art: Two Case Studies. *Langmuir* **2007**, *23* (11), 6396−6403.

(7) Carretti, E.; Fratini, E.; Berti, D.; Dei, L.; Baglioni, P. Nanoscience for Art Conservation: Oil-in-Water Microemulsions Embedded in a Polymeric Network for the Cleaning of Works of Art. *Angew. Chem., Int. Ed.* **2009**, *48* (47), 8966−8969.

DOI: 10.1021/acsami.8b01841
ACS Appl. Mater. Interfaces 2018, 10, 19162−19172

(8) Baglioni, M.; Rengstl, D.; Berti, D.; Bonini, M.; Giorgi, R.; Baglioni, P. Removal of Acrylic Coatings from Works of Art by Means of Nanofluids: Understanding the Mechanism at the Nanoscale. *Nanoscale* **2010**, *2* (9), 1723−1732.
(9) Giorgi, R.; Baglioni, M.; Berti, D.; Baglioni, P. New Methodologies for the Conservation of Cultural Heritage: Micellar Solutions, Microemulsions, and Hydroxide Nanoparticles. *Acc. Chem. Res.* **2010**, *43* (6), 695−704.
(10) Baglioni, M.; Giorgi, R.; Berti, D.; Baglioni, P. Smart Cleaning of Cultural Heritage: A New Challenge for Soft Nanoscience. *Nanoscale* **2012**, *4* (1), 42−53.
(11) Baglioni, P.; Chelazzi, D.; Giorgi, R.; Poggi, G. Colloid and Materials Science for the Conservation of Cultural Heritage: Cleaning, Consolidation, and Deacidification. *Langmuir* **2013**, *29* (17), 5110−5122.
(12) Baglioni, M.; Raudino, M.; Berti, D.; Keiderling, U.; Bordes, R.; Holmberg, K.; Baglioni, P. Nanostructured Fluids from Degradable Nonionic Surfactants for the Cleaning of Works of Art from Polymer Contaminants. *Soft Matter* **2014**, *10* (35), 6798.
(13) Baglioni, P.; Berti, D.; Bonini, M.; Carretti, E.; Dei, L.; Fratini, E.; Giorgi, R. Micelle, Microemulsions, and Gels for the Conservation of Cultural Heritage. *Adv. Colloid Interface Sci.* **2014**, *205*, 361−371.
(14) Baglioni, M.; Berti, D.; Teixeira, J.; Giorgi, R.; Baglioni, P. Nanostructured Surfactant-Based Systems for the Removal of Polymers from Wall Paintings: A Small-Angle Neutron Scattering Study. *Langmuir* **2012**, *28* (43), 15193−15202.
(15) Baglioni, P.; Carretti, E.; Chelazzi, D. Nanomaterials in Art Conservation. *Nat. Nanotechnol.* **2015**, *10* (4), 287−290.
(16) Wolbers, R.; Sterman, N.; Stavroudis, C. *Notes for the Workshop on New Methods in the Cleaning of Paintings*; The Getty Conservation Institute: Marina del Rey, 1988.
(17) Wolbers, R. *Cleaning Painted Surfaces, Aqueous Methods*; Archetype Publications: London, 2000.
(18) Campani, E.; Casoli, A.; Cremonesi, P.; Saccani, I.; Signorini, E. *Quaderni Del Cesmar7: L'Uso Di Agarosio E Agar per La Preparazione Di "Gel Rigidi"—Use of Agarose and Agar for Preparing "Rigid Gels"*, No. 4; Il Prato: Padua, 2007.
(19) Mazzuca, C.; Micheli, L.; Cervelli, E.; Basoli, F.; Cencetti, C.; Coviello, T.; Iannuccelli, S.; Sotgiu, S.; Palleschi, A. Cleaning of Paper Artworks: Development of an Efficient Gel-Based Material Able to Remove Starch Paste. *ACS Appl. Mater. Interfaces* **2014**, *6* (19), 16519−16528.
(20) Micheli, L.; Mazzuca, C.; Cervelli, E.; Palleschi, A. New Strategy for the Cleaning of Paper Artworks: A Smart Combination of Gels and Biosensors. *Adv. Chem.* **2014**, *2014*, 1−10.
(21) Carretti, E.; Grassi, S.; Cossalter, M.; Natali, I.; Caminati, G.; Weiss, R. G.; Baglioni, P.; Dei, L. Poly(vinyl alcohol)−Borate Hydro/Cosolvent Gels: Viscoelastic Properties, Solubilizing Power, and Application to Art Conservation. *Langmuir* **2009**, *25* (15), 8656−8662.
(22) Carretti, E.; Natali, I.; Matarrese, C.; Bracco, P.; Weiss, R. G.; Baglioni, P.; Salvini, A.; Dei, L. A New Family of High Viscosity Polymeric Dispersions for Cleaning Easel Paintings. *J. Cult. Herit.* **2010**, *11* (4), 373−380.
(23) Carretti, E.; Matarrese, C.; Fratini, E.; Baglioni, P.; Dei, L. Physicochemical Characterization of Partially Hydrolyzed Poly(Vinyl Acetate)−Borate Aqueous Dispersions. *Soft Matter* **2014**, *10* (25), 4443−4450.
(24) Baglioni, B.; Berti, D.; Bonini, M.; Carretti, E.; Del Carmen Casas Perez, M.; Chelazzi, D.; Dei, L.; Fratini, E.; Giorgi, R.; Natali, I.; Arroyo, M. C. Gels for the conservation of Cultural Heritage. *MRS Online Proc. Libr.* **2012**, *1418*, 17−26.
(25) Berlangieri, C.; Andrina, E.; Matarrese, C.; Carretti, E.; Traversi, R.; Severi, M.; Chelazzi, D.; Dei, L.; Baglioni, P. Chelators confined into 80pvac-borax highly viscous dispersions for the removal of gypsum degradation layers. *Pure Appl. Chem.* **2017**, *89*, 97−109.
(26) Bonini, M.; Lenz, S.; Giorgi, R.; Baglioni, P. Nanomagnetic Sponges for the Cleaning of Works of Art. *Langmuir* **2007**, *23* (17), 8681−8685.
(27) Bonini, M.; Lenz, S.; Falletta, E.; Ridi, F.; Carretti, E.; Fratini, E.; Wiedenmann, A.; Baglioni, P. Acrylamide-Based Magnetic Nanosponges: A New Smart Nanocomposite Material. *Langmuir* **2008**, *24* (21), 12644−12650.
(28) Pizzorusso, G.; Fratini, E.; Eiblmeier, J.; Giorgi, R.; Chelazzi, D.; Chevalier, A.; Baglioni, P. Physicochemical Characterization of Acrylamide/Bisacrylamide Hydrogels and Their Application for the Conservation of Easel Paintings. *Langmuir* **2012**, *28* (8), 3952−3961.
(29) Yin, L.; Fei, L.; Cui, F.; Tang, C.; Yin, C. Superporous Hydrogels Containing Poly(Acrylic Acid-Co-Acrylamide)/O-Carboxymethyl Chitosan Interpenetrating Polymer Networks. *Biomaterials* **2007**, *28* (6), 1258−1266.
(30) Domingues, J. A. L.; Bonelli, N.; Giorgi, R.; Fratini, E.; Gorel, F.; Baglioni, P. Innovative Hydrogels Based on Semi-Interpenetrating p(HEMA)/PVP Networks for the Cleaning of Water-Sensitive Cultural Heritage Artifacts. *Langmuir* **2013**, *29* (8), 2746−2755.
(31) Bonelli, N.; Chelazzi, D.; Baglioni, M.; Giorgi, R.; Baglioni, P. In *Nanoscience and Cultural Heritage*; Dillmann, P., Bellot-Gurlet, L., Ed.; Atlantis Press: Paris, France, 2016; Vol. *3*, pp 283−311.
(32) Baglioni, M.; Bartoletti, A.; Bozec, L.; Chelazzi, D.; Giorgi, R.; Odlyha, M.; Pianorsi, D.; Poggi, G.; Baglioni, P. Nanomaterials for the cleaning and pH adjustment of vegetable-tanned leather. *Appl. Phys. A: Mater. Sci. Process.* **2016**, *122*, 114.
(33) Barlow, D. J.; Lawrence, M. J.; Zuberi, T.; Zuberi, S.; Heenan, R. K. Small-Angle Neutron-Scattering Studies on the Nature of the Incorporation of Polar Oils into Aggregates of N,N-Dimethyldodecylamine-N-Oxide. *Langmuir* **2000**, *16* (26), 10398−10403.
(34) García, M. T.; Campos, E.; Ribosa, I. Biodegradability and Ecotoxicity of Amine Oxide Based Surfactants. *Chemosphere* **2007**, *69* (10), 1574−1578.
(35) Rathman, J. F.; Christian, S. D. Determination of Surfactant Activities in Micellar Solutions of Dimethyldodecylamine Oxide. *Langmuir* **1990**, *6* (2), 391−395.
(36) Maeda, H.; Muroi, S.; Ishii, M.; Kakehashi, R.; Kaimoto, H.; Nakahara, T.; Motomura, K. Effects of Ionization on the Critical Micelle Concentration and the Surface Excess of Dodecyldimethylamine Oxide in Salt Solutions. *J. Colloid Interface Sci.* **1995**, *175*, 497−505.
(37) Imaishi, Y.; Kakehashi, R.; Nezu, T.; Maeda, H. Dodecyldimethylamine Oxide Micelles in Solutions without Added Salt. *J. Colloid Interface Sci.* **1998**, *197*, 309−316.
(38) Warisnoicharoen, W.; Lansley, A. B.; Lawrence, M. J. Nonionic Oil-in-Water Microemulsions: The Effect of Oil Type on Phase Behaviour. *Int. J. Pharm.* **2000**, *198* (1), 7−27.
(39) Gradzielski, M.; Hoffmann, H. Influence of Charges on Structure and Dynamics of an O/W Microemulsion. Effect of Admixing Ionic Surfactants. *J. Phys. Chem.* **1994**, *98* (10), 2613−2623.
(40) Blanton, T.; Huang, T. C.; Toraya, H.; Hubbard, C. R.; Robie, S. B.; Louer, D.; Gobel, H. E.; Will, G.; Gilles, R.; Raftery, T. JCPDS-International Centre for Diffraction Data Round Robin Study of Silver Behenate. A Possible Low-Angle X-Ray Diffraction Calibration Standard. *Powder Diffr.* **1995**, *10* (2), 91−95.
(41) Gottlieb, M.; Macosko, C. W.; Benjamin, G. S.; Meyers, K. O.; Merrill, E. W. Equilibrium Modulus of Model Poly (Dimethylsiloxane) Networks. *Macromolecules* **1981**, *14* (4), 1039−1046.
(42) MacKintosh, F.; Käs, J.; Janmey, P. Elasticity of Semiflexible Biopolymer Networks. *Phys. Rev. Lett.* **1995**, *75* (24), 4425−4428.
(43) De Gennes, P. G. Scaling Theory of Polymer Adsorption. *J. Phys. (Paris)* **1976**, *37* (12), 1445−1452.
(44) Guenet, J.-M. Structure versus Rheological Properties in Fibrillar Thermoreversible Gels from Polymers and Biopolymers. *J. Rheol.* **2000**, *44* (4), 947.
(45) Pääkkö, M.; Ankerfors, M.; Kosonen, H.; Nykänen, A.; Ahola, S.; Österberg, M.; Ruokolainen, J.; Laine, J.; Larsson, P. T.; Ikkala, O.; Lindström, T. Enzymatic Hydrolysis Combined with Mechanical Shearing and High-Pressure Homogenization for Nanoscale Cellulose Fibrils and Strong Gels. *Biomacromolecules* **2007**, *8* (6), 1934−1941.
(46) Giorgi, R.; Baglioni, M.; Berti, D.; Baglioni, P. New Methodologies for the Conservation of Cultural Heritage: Micellar

DOI: 10.1021/acsami.8b01841
ACS Appl. Mater. Interfaces 2018, 10, 19162−19172

Solutions, Microemulsions, and Hydroxide Nanoparticles. *Acc. Chem. Res.* **2010**, *43* (6), 695−704.
(47) Baglioni, M.; Berti, D.; Teixeira, J.; Giorgi, R.; Baglioni, P. Nanostructured Surfactant-Based Systems for the Removal of Polymers from Wall Paintings: A Small-Angle Neutron Scattering Study. *Langmuir* **2012**, *28* (43), 15193−15202.
(48) Liu, Y. C.; Baglioni, P.; Teixeira, J.; Chen, S. H. Structure and Interaction of Lithium Dodecyl Sulfate Micelles in the Presence of Li-Specific Macrocyclic Cage: A Study by SANS. *J. Phys. Chem.* **1994**, *98* (40), 10208−10215.
(49) Bockstahl, F.; Duplâtre, G. Effect of 1-Pentanol on Size and Shape of Sodium Dodecyl Sulfate Micelles as Studied by Positron Annihilation Lifetime Spectroscopy. *J. Phys. Chem. B* **2001**, *105* (1), 13−18.
(50) Sheu, E. Y.; Chen, S. H. Thermodynamic Analysis of Polydispersity in Ionic Micellar Systems and Its Effect on Small-Angle Neutron Scattering Data Treatment. *J. Phys. Chem.* **1988**, *92* (15), 4466−4474.
(51) Hayter, J. B.; Penfold, J. An Analytic Structure Factor for Macroion Solutions. *Mol. Phys.* **1981**, *42* (1), 109−118.
(52) Liu, Y. C.; Ku, C. Y.; LoNostro, P.; Chen, S. H. Ion Correlations in a Micellar Solution Studied by Small-Angle Neutron and X-Ray Scattering. *Phys. Rev. E: Stat. Phys., Plasmas, Fluids, Relat. Interdiscip. Top.* **1995**, *51* (5), 4598−4607.
(53) Zana, R. Aqueous Surfactant-Alcohol Systems: A Review. *Adv. Colloid Interface Sci.* **1995**, *57* (Suppl C), 1−64.
(54) Baglioni, M.; Jàidar Benavides, Y.; Berti, D.; Giorgi, R.; Keiderling, U.; Baglioni, P. An Amine-Oxide Surfactant-Based Microemulsion for the Cleaning of Works of Art. *J. Colloid Interface Sci.* **2015**, *440*, 204−210.
(55) Palazzo, G.; Fiorentino, D.; Colafemmina, G.; Ceglie, A.; Carretti, E.; Dei, L.; Baglioni, P. Nanostructured Fluids Based on Propylene Carbonate/Water Mixtures. *Langmuir* **2005**, *21* (15), 6717−6725.
(56) Derrick, M. Fourier Transform Infrared Spectral Analysis of Natural Resins Used in Furniture Finishes. *J. Am. Inst. Conserv.* **1989**, *28* (1), 43−56.
(57) Gunasekaran, S.; Anbalagan, G.; Pandi, S. Raman and Infrared Spectra of Carbonates of Calcite Structure. *J. Raman Spectrosc.* **2006**, *37* (9), 892−899.
(58) Miyoshi, T. Fluorescence from Resins for Oil Painting Under N_2 Laser Excitation. *Jpn. J. Appl. Phys.* **1990**, *29* (9), 1727−1728.
(59) Nevin, A.; Comelli, D.; Osticioli, I.; Toniolo, L.; Valentini, G.; Cubeddu, R. Assessment of the Ageing of Triterpenoid Paint Varnishes Using Fluorescence, Raman and FTIR Spectroscopy. *Anal. Bioanal. Chem.* **2009**, *395* (7), 2139−2149.
(60) Pelagotti, A.; Pezzati, L.; Bevilacqua, N.; Vascotto, V.; Reillon, V.; Daffara, C. A Study of UV Fluorescence Emission of Painting Materials. *Art '05−8th International Conference on Non-Destructive Investigations and Microanalysis for the Diagnostics and Conservation of the Cultural and Environmental Heritage. Lecce, Italy* **2005**, A97.
(61) Garside, P.; Wyeth, P. Identification of Cellulosic Fibres by FTIR Spectroscopy: Thread and Single Fibre Analysis by Attenuated Total Reflectance. *Stud. Conserv.* **2003**, *48* (4), 269−275.

DOI: 10.1021/acsami.8b01841
ACS Appl. Mater. Interfaces 2018, 10, 19162−19172